

Electrosynthesis of polyquinone nanowires with dispersed platinum nanoparticles toward formic acid oxidation

M. A. del Valle¹ · L. A. Hernández² · A. M. Ramírez¹ · F. R. Díaz¹

Received: 9 June 2016 / Revised: 25 July 2016 / Accepted: 2 August 2016 / Published online: 13 August 2016
© Springer-Verlag Berlin Heidelberg 2016

Abstract Conducting polymer nanostructuring enables a substantial improvement of many electro-catalytic processes, e.g., formic acid (HCOOH, FA) electro-oxidation. In this case, a stainless steel (SS) electrode is first modified with poly(1-amino-9,10-anthraquinone-*co-o*-phenylenediamine) (COP) and then, by means of a template that can be chemically removed, poly(1-amino-9,10-anthraquinone) nanowires (PIAAQnw) are electro-synthesized; this procedure has allowed the effective FA electro-catalytic oxidation generating adsorbed CO, which is quickly converted to CO₂. Subsequently, when platinum nanoparticles (dispersed by electro-chemical techniques) are also incorporated on the polymeric nanowires, oxidation peaks are observed at ca. 1000 mV, with a current increase up to fourfold. In this way, the method provides a highly reproducible nanostructured

electrode that is prepared solely by electro-chemical techniques offering promising results for FA electro-catalytic oxidation.

Keywords Formic acid · Electro-oxidation · Polymer nanowires · Poly(1-amino-9,10-anthraquinone) · Nanowire electrosynthesis

Introduction

Research related to the use of HCOOH (formic acid (FA)) has increased significantly in recent years due to its high-efficiency power conversion, easy transportation, and storage, and because it offers a clean and sustainable alternative [1, 2]. Thus, the FA electro-oxidation using different metals at macroscopic and nanometric level promoted the early research in this field [3]. As a result of its high activity, platinum is the most used electro-catalyst anode [4, 5], however, nowadays its use has decreased because, in addition to high production costs and low durability [4, 6], it is rapidly poisoned during the oxidation processes.

The FA electro-oxidation processes to obtain CO₂ require the breaking of two FA molecule bonds, namely OH and CH. Breaking the OH fragment is relatively easy, owing to the acid-base equilibrium inherent to FA, but the second breakdown requires high affinity and specificity of the electrode used as anode, favoring hydrogenation and subsequent dehydration of the electrode, being platinum, as already mentioned, the one with the highest efficiency. By this route, when metal-based electrodes are used, the formation of CO_(ads) at low potential can be observed; this interaction is very strong and difficult to break, leading ultimately to CO₂ that requires the transfer of an OH group in the process. This path is known as

✉ M. A. del Valle
mdvalle@uc.cl

L. A. Hernández
lahernandez@uc.cl

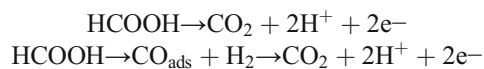
A. M. Ramírez
aaramirez@uc.cl

F. R. Díaz
fdiaz@uc.cl

¹ Facultad de Química, Departamento de Química Inorgánica, Laboratorio de Electroquímica de Polímeros (LEP), Pontificia Universidad Católica de Chile, Vicuña Mackenna 4860, 7820436, Macul, Santiago, Chile

² Facultad de Ciencias, Instituto de Química y Bioquímica, Laboratorio de Electroquímica, Universidad de Valparaíso, Gran Bretaña 1111, Playa Ancha, Valparaíso, Chile

the direct oxidation pathway whose reaction mechanism is not yet fully elucidated [7]:



As mentioned, one of the main disadvantages in using Pt or other metal-based electrodes is the poisoning as the reaction proceeds, losing its activity as is reused; therefore, it has been sought to conjugate the properties of other systems in such a way that the synergy of the combination of these materials with metal nanoparticles helps to enhance efficiency and reduce platinum poisoning.

Recently, Pt composites with conducting polymers (CPs) [8–11], such as polythiophene [12, 13], polyaniline [14], polypyrrole [15], among others, have been employed to study FA electro-catalysis, based on the advantages that CPs present, e.g., large surface area and high chemical and environmental stability, in addition to the synergistic effect that occurs between CPs and Pt particles [16–19]. New technologies and advances in this area, which allow nanostructuring-forming nanocomposites with templates [8–10], have considerably broadened the already known yield of bulky polymers [8, 11].

In the current paper, electrodes modified with polymeric nanostructures previously reported by us [12, 13] will be tested. The assembly consists of poly(1-amino-9,10-anthraquinone) P1AAQ conducting polymer nanowires (P1AAQnw), electro-synthesized on a poly(1-amino-9,10-anthraquinone-*co-o*-phenylenediamine) (COP) electrode using stainless steel (SS) as substrate. To this purpose, a SiO₂ template (tp) that guides the growth of the nw was electro-deposited on the COP; the tp is subsequently chemically removed [14]. Next, through an electro-chemical method also developed and checked by our group [11], incorporation of dispersed platinum nanoparticles (Ptnp) on these modified electrodes (SS|COP-P1AAQnw-Ptnp) is performed (Fig. 1). The assembly was further evaluated respect to FA electro-oxidation. Hence, if the activity were favored, the costs associated with this type of anodes would be lowered, enabling an important breakthrough for this kind of fuel cells. Another important

advantage of this system is the preparation of nanostructures (polymer and Pt) in situ, directly upon the electrode, which ensures reproducibility that is almost impossible to achieve if nanoparticles are synthesized ex situ and subsequently placed over the substrate.

Materials and methods

SS electrode modification with COP (SS|COP) followed by template deposition (SS|COP-Tp)

All solutions were prepared with fresh Milli-Q grade water obtained from a Heal Force (Smart Series) deionizer. The experiments were conducted at room temperature (20 °C) under a high purity argon atmosphere in a three-compartment, three-electrode anchor-type electro-chemical cell. A 0.07-cm² geometric area steel (AISI 316) disk (SS) was used as working electrode, and a platinum wire coil of large geometric area was the counter electrode. Ag|AgCl in a solution of tetramethylammonium chloride, whose potential matched that of a saturated calomel electrode (SCE), was the reference electrode [15]. The monomers used in the electrosynthesis were 1AAQ (98 %, Aldrich) and *o*-phenylenediamine (OPD) (99.5 %, Aldrich), which were prepared following the protocols reported elsewhere [16]. The template was prepared in an ethanol (98 %) Milli-Q water (50 % v/v) mixture containing 0.05 mol L⁻¹ of potassium nitrate (KNO₃, Aldrich) as supporting electrolyte, 0.0034 mol L⁻¹ tetraethyl orthosilicate (TEOS, Aldrich) as precursor of silicon oxide (SiO₂), and 0.115 mol L⁻¹ hexadecyltrimethylammonium bromide (CTAB, Aldrich) as surfactant, by applying -1.400 V for 5 s, and then dried 12 h at 130 °C.

P1AAQnw electrosynthesis on SS|COP-Tp [17]

The P1AAQnw-modified electrodes (SS|COP-P1AAQnw) have been obtained on SS|COP-Tp-modified electrodes, applying 1100 mV during 40 s to the SS|COP-Tp

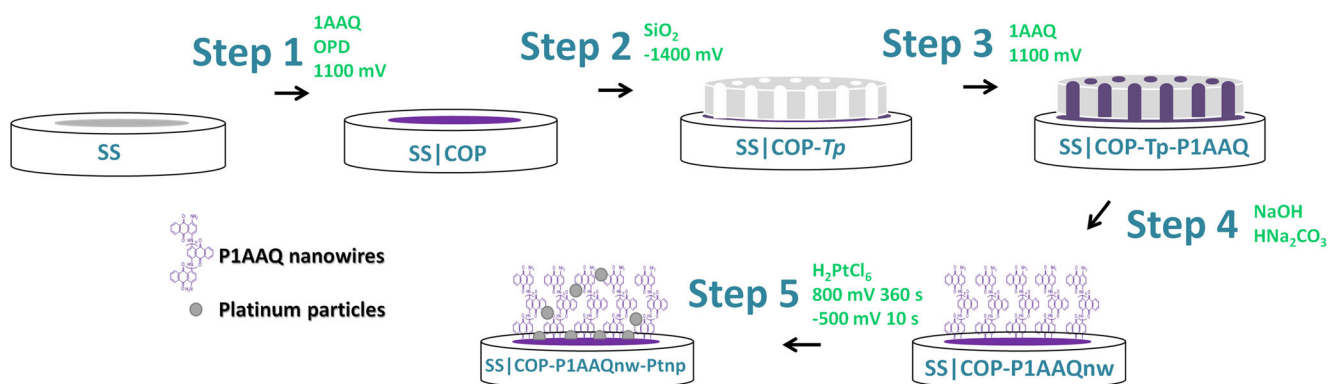


Fig. 1 Scheme to obtaining SS|COP-P1AAQnw-Ptnp

electrode immersed into 0.01 mol L⁻¹ 1AAQ solution; subsequently, they were dried during 12 h at room temperature. Removal of SiO₂ template from SS|COP-1AAQnw electrodes was accomplished using 0.1 mol L⁻¹ NaOH (99.0 %, Merck) solution; to this purpose, 10 μL was deposited on each electrode and allowed to stand 10 min. The solution was then neutralized and the electrode washed with 5 % w/w NaHCO₃ (99 %, Merck). This extraction procedure is repeated twice for each device.

Ptnp dispersion over the SS|COP-1AAQnw-modified electrode

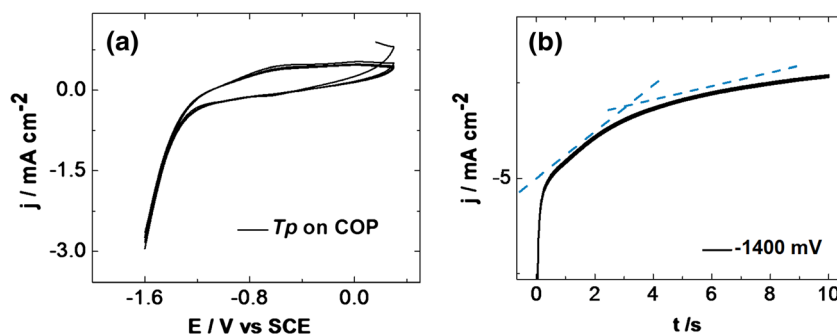
Electrosynthesis of Ptnp dispersed on P1AAQnw follows the designed and previously reported methodology. Therefore, a 0.001 mol L⁻¹ of chloroplatinic acid (H₂PtCl₆) + 0.1 mol L⁻¹ potassium hexafluorophosphate (KPF₆) supporting electrolyte aqueous solutions was utilized. The dispersion is conducted using what we called 1 platinization cycle (PC) and consists of a methodology based on the *p*-doping process of conducting polymers: a fixed potential of 0.800 V is applied during 360 s to produce the *p*-doping from the anion provided by the acid, i.e., PtCl₆²⁻, and immediately the potential is set at -0.500 V for 10 s to reduce Pt(IV) that will become incorporated into the polymer matrix as Ptnp. Thus, the SS|COP-nw-Pt-modified electrode is obtained.

To assess FA electro-oxidation, solutions in the concentration range 0.1–8.0 mol L⁻¹ FA (99.0 %, Merck) + 0.1 mol L⁻¹ KPF₆ (supporting electrolyte) were utilized.

Instruments

All electro-chemical measurements were carried out on a CH Instruments Electro-chemical Workstation. Images from the electrode surface (scanning electron microscope (SEM)) were obtained on an LEO VP1400 SEM and on a Hitachi HF2000-FEG transmission electron microscope (TEM), using carbon-coated nickel grids.

Fig. 2 **a** Voltammetric profiles during template electro-obtainment on COP; **b** *j*/*t* transient during template electrodeposition on SS-modified copolymer (SS|COP-Tp). Interfaces: SS|0.0034 mol L⁻¹ TEOS, +0.115 mol L⁻¹ CTAB, +0.05 mol L⁻¹ KNO₃ in ethanol/Milli-Q water (50 % v/v) mixture. *v* = 50 mV s⁻¹



Results and discussion

Optimization of template electro-obtainment on the copolymer

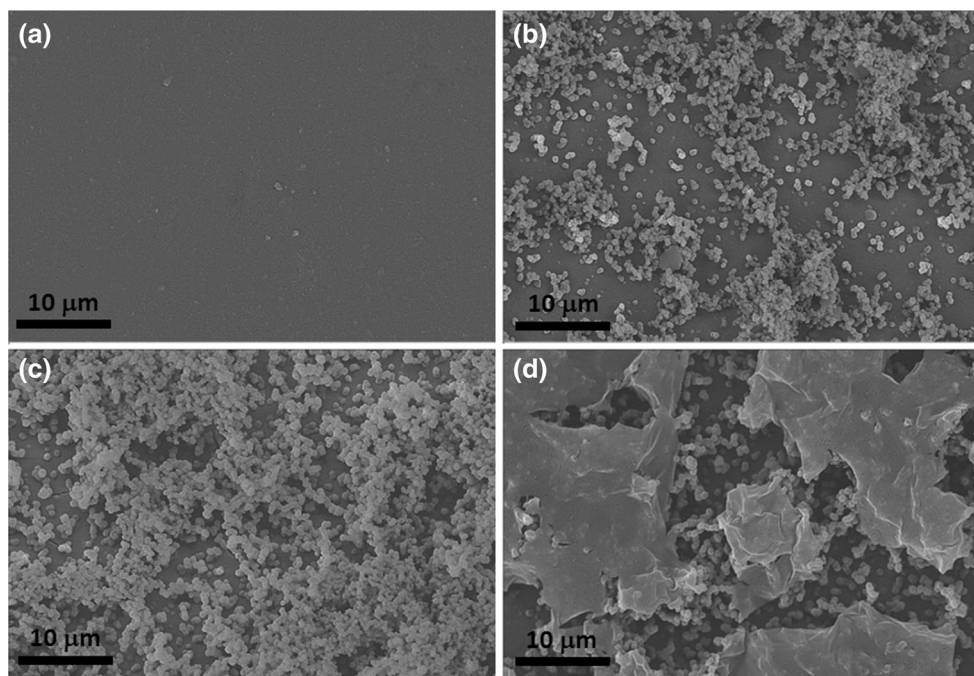
Template preparation on SS|COP by cyclic voltammetry and chronoamperometry

The template electro-chemical preparation was conducted on a COP previously modified SS electrode by adapting methods reported elsewhere [10, 16]. Cyclic voltammograms (CV) (Fig. 2a) were recorded within a 0.300 and -1.600 V window. After drying (130 °C, 12 h), a very homogeneous and temperature resistant white coating was obtained. The successful obtainment of SiO₂ upon the copolymer was predictable from AFM morphological characterization [16], wherein the formation of a homogeneous, very uniform, low roughness, and good conductivity deposit was verified.

Chronoamperometric (potentiostatic method (PM)) study of template electro-preparation on the COP was performed applying potentials from -1.500 to -1.200 V for 10 s. In this case, a homogeneous coating over the copolymer-modified electrode was achieved only at -1.400 V; therefore, this potential was chosen as the most suitable for template electrosynthesis. Thus, a continuous current increase was observed as the potential was applied.

The early signs concerning the optimal time for obtaining a permeable mesoporous film of template, which permits subsequent electrodeposition of P1AAQ in the confined spaces of their pores, were inferred from the recorded transient (Fig. 2b) that showed a slope variation at about 4 s of electrolysis. This current variation can be ascribed to surface area change, since at the early seconds of electro-obtainment, SiO₂ growth would have been generated into the free space left by the surfactant that at negative potentials become compacted as micelle. After polymer growth has reached a height that exceeds the micelle height, the polymer starts growing on it and then grows upon itself, generating the observed slope change during the electro-preparation.

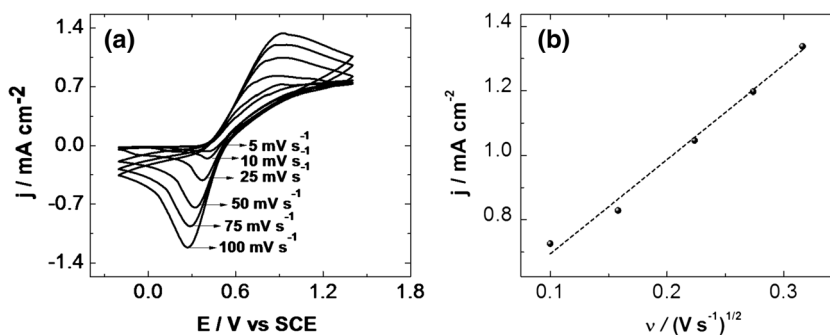
Fig. 3 SEM images of template prepared upon COP by PM at -1.400 V during **a** 4, **b** 5, **c** 7, and **d** 10 s



Following the proper potential optimization for electro-preparation of suitable SiO_2 template using PM, the right time to completely coat the electrode and in addition to have a permeable film was surveyed. Assays were conducted during 4, 5, 7, and 10 s, observing that as time increases, it is visible at a glance that the coating upon the electrode surface is increasingly covering more area over the modified electrode but at the same time becomes less homogeneous. SEM images (Fig. 3) allowed corroborating that at longer times (Figs. 3c, d) the small heterogeneous spheres grow in volume and uniformity over the electrode, until the surfactant guided mesopores are covered, leading to obtaining an insulator electrode.

For 4 s of electrolysis, a great amount of heterogeneous spheres is not observed by SEM, and the electrode coating reproducibility is no good, hence this time was disregarded for template preparation. Instead, 5 s (Fig. 3b) of electro-preparation was selected to work, because the coating over the modified electrode is total, despite what it could be inferred from SEM images.

Fig. 4 **a** Rate study for obtaining the effective area of the SS|COP-Tp; **b** diffusion coefficient determination. Interfaces: SS|COP-Tp 0.01 mol L^{-1} ferrocene, $+0.1 \text{ mol L}^{-1}$ TBAPF₆ in CH_3CN



Permeability, diffusion coefficient, and effective area of the working electrode with the template upon the COP

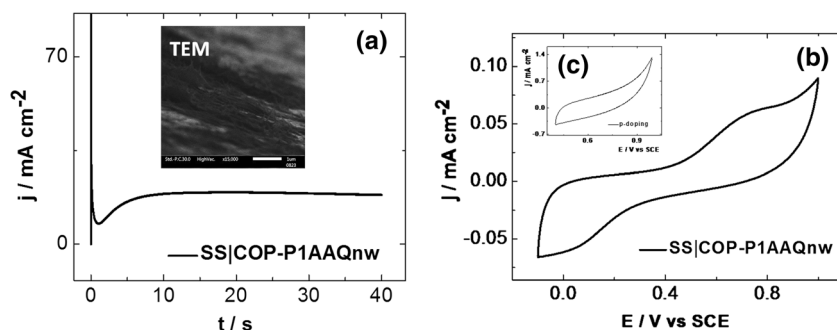
The permeable film of SiO_2 obtained was evaluated by CV of the modified electrodes using the well-defined ferrocene/ferrocenium redox couple. At the same time, this response was utilized to assess the effective area of the working electrode, considering that when nw are electro-synthesized within the template, they remain attached to the copolymer, leaving an effective area that must be recalculated. To this purpose, the Randles-Sevcik Eq. (1) [17, 18] was used:

$$I_p = K \cdot n^{3/2} \cdot A \cdot \sqrt{D \cdot \nu} \cdot C \quad (1)$$

where I_p is the oxidation peak current, K a constant equal to $2.69 \times 10^5 \text{ C mol}^{-1} \text{ v}^{-1/2}$, n number of electrons involved in the redox reaction, A electrode area (cm^2), D diffusion coefficient of the analyte ($\text{cm}^2 \text{ s}^{-1}$), C concentration (mol cm^{-3}), and ν scan rate (V s^{-1}).

A ν study between 5 and 100 mV s^{-1} (Fig. 4a) revealed that the slope (m) of the plot in Fig. 4b enables recalculating the

Fig. 5 **a** j/t transients obtained during nw electrosynthesis on SS|COP-Tp and TEM images of SS|COP-P1AAQnw; **b** P1AAQnw electro-chemical response in 1×10^{-4} mol L $^{-1}$ KPF $_6$, $\nu = 100$ mV s $^{-1}$; **c** P1AAQnw p -doping in 10^{-1} mol L $^{-1}$ KPF $_6$, $\nu = 100$ mV s $^{-1}$



effective area when the template is present, taking ferrocene diffusion coefficient = 2.60×10^{-9} cm 2 s $^{-1}$ [19]. The calculated electrode area was 3.41×10^{-3} cm 2 that corresponds to a decrease equal to one order of magnitude with respect to the geometric area of the SS substrate.

Electro-preparation of P1AAQnw and Ptnp dispersion

Electrosynthesis of P1AAQnw was accomplished by PM directly on the already electro-synthesized template [14]. Figure 5a illustrates a continuous current growth of the respective j/t transient that, after 25 s, starts declining; this could mean that the polymer is filling the mesopores. Polymer behavior in KPF $_6$ after template removal is seen in Fig. 5b, from where the proper oxidation potential (p -doping process, Fig. 5c) can be also worked out, being possible to deduce that 0.800 V is the most appropriate potential to dope the obtained polymer.

Thus, when 0.800 V is applied, thanks to the p -doping process of the nanostructured polymer, PtCl $_6^{2-}$ inclusion inside the P1AAQnw is favored. Then, all what is needed is to apply a reduction potential for a short period of time to achieve reduction and homogenous dispersion of Ptnp into the polymeric matrix [12]. The corresponding voltammetric response is depicted in Fig. 5.

If the P1AAQnw electro-chemical responses are compared before and after the addition of Ptnp (Fig. 6), two oxidation peaks are observed at 0.120 and 0.500 V

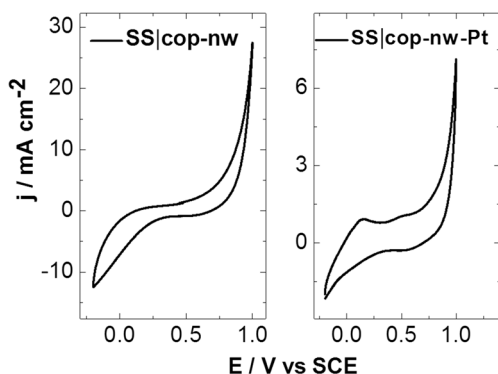
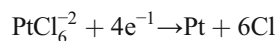


Fig. 6 SS|COP-P1AAQnw and SS|COP-P1AAQnw-Ptnp voltammetric profile in 0.1 mol L $^{-1}$ H $_2$ SO $_4$ + 10^{-1} mol L $^{-1}$ KPF $_6$, $\nu = 100$ mV s $^{-1}$

when Ptnp was incorporated, as already corroborated by polymers having very similar structures and Ptnp dispersed over its surface [20]. This, together with TEM micrographs (Fig. 7), would demonstrate that the proposed modification has been successfully accomplished.

Figure 7 shows a representative image and nanoparticles size of Pt. It can be seen that Ptnp are dispersed over SS|COP-P1AAQnw with average particle size of 20 nm (d_{TEM} ; Table 1). Deposited Pt mass was calculated by integration of the electrical charge consumed during the deposition process Q (C cm $^{-2}$), assuming that the only contributing reaction was the faradaic process [21]:



Then, the quantity of platinum on the electrode (w) is calculated from:

$$w = Q \cdot M / (z \cdot F) \quad (2)$$

where M is Pt molar mass (195.09 g mol $^{-1}$), z number of exchanged electrons, and F the Faraday constant (96,485.3 C mol $^{-1}$). Then, the Pt deposited on P1AAQ nanowires was 5.7 mg cm $^{-2}$.

Formic acid electro-oxidation on the modified electrodes

In Fig. 8a, the electro-oxidation of FA during the last two stages of electrode manufacturing is observed; hence it was demonstrated that although the inclusion of P1AAQnw allows

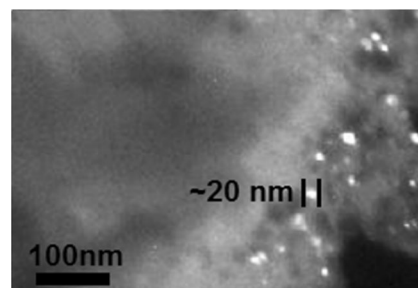


Fig. 7 TEM micrographs of Ptnp dispersed on the SS|COP-P1AAQnw electrode

Table 1 Physical characteristics of SS|COP-P1AAQnw-Ptnp

Q_o (mC cm ⁻²)	Q_i (mC)	Pt loading w (g cm ⁻²)	True surface area A_r (mC m ²)	Specific surface area S (m ² g ⁻¹)	Particle size d (nm)	Particle size d_{TEM} (nm)
45.6	0.2	5.7	3.4 ^a	1.7	16	~20

^a Determined from CO_{ads} on Ptnp

obtaining an effective electro-catalysis, Ptnp inclusion improves even more the electro-catalytic process, since a significant current increase is evidenced.

In the voltammetric profiles shown in Fig. 8a, it is also interesting to note just one oxidation peak (~1000 mV), which would account for a very high reaction kinetics for the electro-oxidation process on SS|COP-P1AAQnw-Ptnp, or else, that due to the large increase in effective area, given by the P1AAQ nano-structuring and Ptnp inclusion, oxidation of the entire FA molecules on the electrode surface would be possible, without resulting in electro-chemically detectable CO_{ads} adsorption generated during this catalytic process [22, 23].

In Fig. 8b, the possible uses of each electrode obtained in the electro-oxidation, using SS|COP and SS|COP-Tp with and without Ptnp incorporation were analyzed during the manufacturing process, which allowed verifying that, since low currents were observed, none of these would be effective for the electro-catalysis. Anyway, SS|COP is the electrode exhibiting the best electro-catalytic response, possibly due to the low roughness of the copolymer that allows effective CO_{ads} adsorption. On the other hand, the template provides a very small surface area (as inferred from potential scan rate studies), which prevents any electro-catalysis. Ptnp inclusion enables observing small currents for both electrodes but always lower than those already found for the nanostructured copolymer.

Thus, it is possible to corroborate that the incorporation of nw and Ptnp significantly improves the current response during electro-oxidation (twofold), showing better response than those reported in similar works under analogous working conditions [20, 21].

If the effect of concentration on the SS|COP-P1AAQnw-Ptnp optimized electrode is analyzed (Fig. 9a), it can be seen how, with increasing concentration, the electro-oxidation profile is maintained only until concentrations ≤ 6 mol L⁻¹. At very high concentrations (6 and 8 mol L⁻¹), while the electrode is not poisoned, the voltammetric profile starts disappearing. If the potential window for both concentrations (Fig. 9b) is expanded, the profile similarity with other previously reported by several authors [12, 20] can be revealed. They observed CO_{ads} adsorption proving that at high concentrations (≥ 6 mol L⁻¹) oxidation to CO_2 , due to saturation of the system, would not be direct, preventing the swift release and conversion of FA into CO_2 , accumulating thus CO_{ads} molecules on the Ptnp surface. Nevertheless, at lower concentrations (Fig. 9a), FA direct oxidation to CO_2 indeed would take place.

From the results of FA electro-oxidation in Fig. 8a, it is also possible to conduct a more thorough analysis of the effective area of Ptnp on the SS|COP-P1AAQnw-Ptnp surface, based on the information reported by Gloaguen et al. [24]. Since increase of electro-catalytic activity seemed to be enhanced by the inclusion of Ptnp and this in turn depends on the number of available surface sites, the activity referred to the platinum surface area (A_r), has a great physical significance. To obtain it, integration is first necessary to determine the area under the voltammetric profiles recorded on SS|COP-P1AAQnw and SS|COP-P1AAQnw-Ptnp; then, from its subtraction, is possible to calculate the actual charge (Q_i), corresponding to what has been carried out just on the Ptnp, assuming that each platinum atom should interact with at least one CO_{ads} . In this case, an actual Q of 3.18 mC cm⁻² was found.

Fig. 8 FA oxidation voltammograms on (a) SS|COP-P1AAQnw and SS|COP-P1AAQnw-Ptnp and (b) SS|COP, SS|COP-Ptnp, and SS|COP-(Tp)-Ptnp in 0.1 mol L⁻¹ formic acid solution. $\nu = 50$ mV s⁻¹

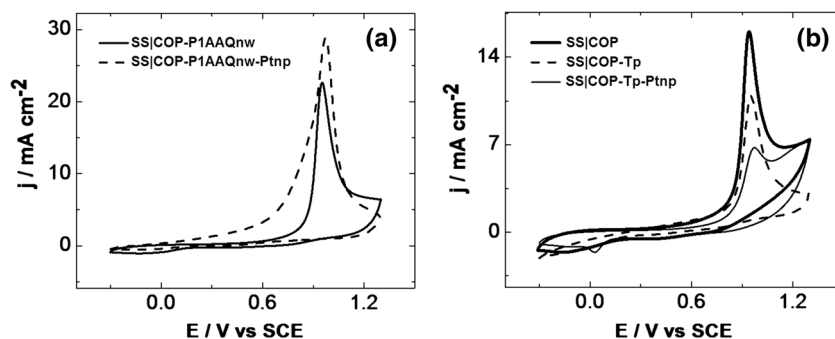
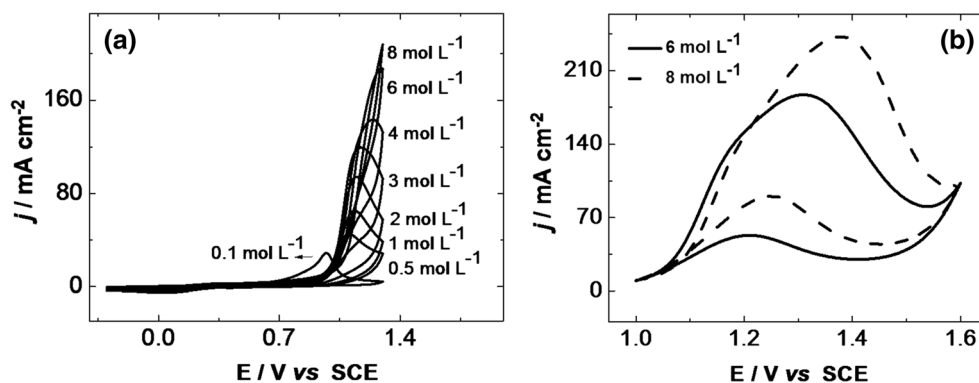


Fig. 9 **a** Voltammetric profile during FA electro-oxidation at different concentrations on SS|COP-nw-Pt; **b** enlargement of the working window for FA electro-oxidation at higher concentrations on SS|COP-nw-Pt. $\nu = 50 \text{ mV s}^{-1}$



Equation 3 enables establishing the amount of Ptnp atoms that have effectively participated in the electro-catalysis:

$$Q_r(\text{mC})/\text{real cm}^2 = F \cdot n/N \tag{3}$$

where N is the Avogadro's constant (6.022×10^{23} atoms mol^{-1}), which yields 1.99×10^6 platinum atoms cm^2 .

On the other hand, the Pt area (A_r , cm^2) can be calculated through the relationship between charges Q_r and the corresponding charge obtained from the working current (Q_c), i.e., $A_r = Q_c/Q_r$, thereby it is possible to determine the specific surface area (S) in $\text{m}^2 \text{g}^{-1}$ according to Eq. 4:

$$S = 100 A_r / (W \cdot A_g) \tag{4}$$

This enables a macroscopic idea of the amount of Pt that effectively acts on the electro-catalysis, different from the actual amount, which is deposited on the electrode surface, disregarding an idea of the Ptnp morphology. Hence, applying a structural model to S , aided by the TEM images (Fig. 7), and assuming that Pt particles are highly homogeneous and with spherical shape, dispersed uniformly over the electrode surface, the electrode area A_g , where Ptnp ($3.41 \times 10^{-3} \text{ C m}^2$) have been electro-deposited, particle size (d) (nm) is then calculated from:

$$d = 6000 / (\rho \cdot S) \tag{5}$$

where ρ is the platinum density (21.04 g cm^{-3}), obtaining a theoretical average particle size of ca. 16 nm, which is consistent with the $\sim 20 \text{ nm}$ worked out from TEM (Fig. 6; Table 1) images.

Kinetic features of FA electro-oxidation on SS|COP-P1AAQnw-Ptnp electrode

Figure 10 shows a current density (j) vs. potential scan rate (ν) plot for FA electro-oxidation on SS|COP-P1AAQnw-Ptnp, wherein it can be verified that the current density of the anodic

peak is directly proportional to the square root of the scan rate, indicating a diffusion controlled process [25].

SS|COP-P1AAQnw-Ptnp stability depending on the concentration

SS|COP-P1AAQnw-Ptnp electrode stability was measured by comparing the anodic peak of FA electro-oxidation using 0.1 and 8 mol L^{-1} solutions, after 100 successive electro-oxidation cycles and can be seen in Figs. 11a, b, respectively.

These results using the same electrode indicate that the stability of the electrode during the continuous cycling of electro-catalysis presents lower standard deviation when working at lower FA concentrations ($\sigma_{0.1M}$ 1.03×10^{-6} and 1.08×10^{-4} , respectively). The results also confirm what it has been already mentioned namely that at low concentrations, poisoning of the electrode would not occur, but the poisoning indeed takes place when greater FA concentrations are used. In this case, as noted, the CO adsorption on SS|COP-P1AAQnw-Ptnp surface is so high, which does not allow a reliable reuse of the electrode over 20 cycles, where the standard deviation is $\leq 10^{-5}$, showing a decrease of the catalytic activity, which is also evidenced by smaller currents.

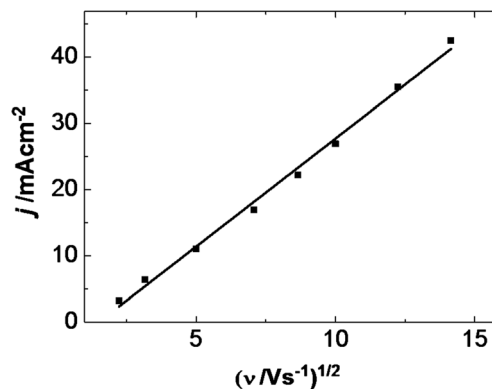
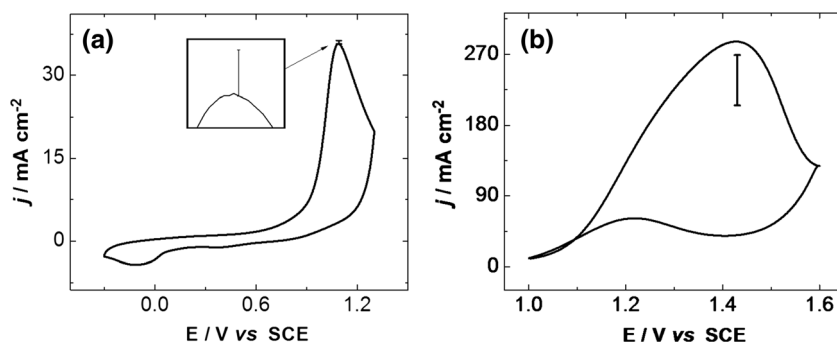


Fig. 10 Anodic peak current vs. scan-rate square root plot of FA oxidation on SS|COP-P1AAQnw-Ptnp in 0.1 mol L^{-1} formic acid + 0.1 mol L^{-1} KPF_6 aqueous solution

Fig. 11 Electro-chemical response and standard deviation of SS|COP-P1AAQnw-Ptnp in FA: (a) 0.1 mol L^{-1} , (b) 8 mol L^{-1} FA. $\nu = 100 \text{ mV s}^{-1}$



It is noteworthy, finally, that the use of electro-chemical techniques for each of the steps of the electrode modification guarantee variables control and reproducibility, particularly when generating nanostructures in situ, phenomenon practically impossible when the modified electrodes are prepared adding nanostructures synthesized ex situ. In that case, it is very difficult to control that the surface be perfectly reproducible, as verified by previous studies concerning the characterization of the electrodes prepared and used in the current work [24].

Conclusions

Optimization of the SiO_2 template electro-chemical obtaining on COP allowed the successful electrosynthesis of P1AAQnw on an SS-modified electrode. Template speed studies allowed the effective working area to be determined, this being $3.41 \times 10^{-3} \text{ cm}^2$.

The prepared P1AAQnw showed a *p*-doping response that enabled Ptnp, dispersion. Furthermore, voltammetric response and TEM micrographs of these electrodes corroborated the inclusion of the metallic nanoparticles ($\sim 20 \text{ nm}$) over the P1AAQnw. It was also corroborated from the theoretical treatment of the charges, which yielded Ptnp sizes of 16 nm .

Evaluation of the effective FA electro-oxidation demonstrated the considerable improvement obtained when the polymer is nanostructured, becoming evident an increase of the anodic peak current ($\sim 1000 \text{ mV}$) that increased even more, ca. twofold, when Ptnp was dispersed.

The systematic study of FA electro-oxidation at concentrations $\leq 6 \text{ mol L}^{-1}$ does not possess the characteristic profile of CO adsorption due to rapid reaction kinetics on the electrode; however, at FA concentrations $\geq 6 \text{ mol L}^{-1}$, typical profiles of CO adsorption is observed as a result of system saturation. These results were also consistent when the stability of the electrode was studied, showing that at low concentrations the variability of CO oxidation peak current is favored, which does not occur at high concentrations wherein reproducible

FA electro-oxidation peak currents are not possible to be obtained.

Furthermore, the potential scan rate study showed that FA electro-oxidation on SS|COP-P1AAQnw-Ptnp is a diffusion-controlled process.

Thus, this method provides a highly reproducible nanostructured electrode that is prepared solely based on electro-chemical techniques and offers promising results for FA electro-catalytic oxidation.

Acknowledgments Funding through FONDECYT Project 1141158 is kindly acknowledged.

References

- Zhang X, Zhang B, Liu D, Qiao J (2015) One-pot synthesis of ternary alloy CuFePt nanoparticles anchored on reduced graphene oxide and their enhanced electrocatalytic activity for both methanol and formic acid oxidation reactions. *Electrochim Acta* 177:93–99
- Chen D, Cui P, Liu H, Yang J (2015) Heterogeneous nanocomposites composed of silver sulfide and hollow structured Pd nanoparticles with enhanced catalytic activity toward formic acid oxidation. *Electrochim Acta* 153:461–467
- Wang L, Zhai J-J, Jiang K, Wang J-Q, Cai W-B (2015) Pd–Cu/C electrocatalysts synthesized by one-pot polyol reduction toward formic acid oxidation: structural characterization and electrocatalytic performance. *Inter J Hydrogen. Energy* 40:1726–1734
- Jeon H, Jeong B, Choun M, Lee J (2014) In-situ electrochemical extended X-ray absorption fine structure spectroscopy study on the reactivation of Pd electrocatalyst in formic acid oxidation. *Electrochim Acta* 140:525–528
- Gojuki T, Numata Y, Mukouyama Y, Okamoto H (2014) Hidden negative differential resistance in the oxidation of formic acid on platinum. *Electrochim Acta* 129:142–151
- Al-Akraa IM, Mohammad AM, El-Deab MS, El-Anadouli BE (2015) Electrocatalysis by design: synergistic catalytic enhancement of formic acid electro-oxidation at core-shell Pd/Pt nanocatalysts. *Inter J Hydrogen. Energy* 40:1789–1794
- Perales-Rondón JV, Herrero E, Feliu JM (2015) On the activation energy of the formic acid oxidation reaction on platinum electrodes. *J Electroanal Chem* 742:90–96
- del Valle MA, Salgado R, Armijo F (2014) PEDOT nanowires and platinum nanoparticles modified electrodes to be assayed in formic acid electro-oxidation. *Int J Electrochem Sci* 9:1557–1564
- del Valle MA, Ramos AC, Antilen MP, Hernandez LA, et al. (2014) Electro-synthesis and characterization of polymer nanostructures

- from terthiophene using silica mesoporous films as template. *Electrochim Acta* 53:146–151
10. Walcarius A, Sibottier E, Etienne M, Ghanbaja J (2007) Electrochemically assisted self-assembly of mesoporous silica thin films. *Nat Mater* 6:602–608
 11. del Valle MA, Gacitúa M, Díaz FR, et al. (2009) Electrosynthesis of polythiophene nanowires via mesoporous silica thin film templates. *Electrochim Commun* 11:2117–2120
 12. del Valle MA, Gacitúa M, Díaz FR, Armijo F, Soto JP (2012) Electrosynthesis and characterization of polythiophene nano-wires/platinum nano-particles composite electrodes. Study of formic acid electrocatalytic oxidation. *Electrochim Acta* 71:277–282
 13. Hernández LA, del Valle MA, Armijo F (2016) Electrosynthesis and characterization of nanostructured polyquinone for use in detection and quantification of naturally occurring dsDNA. *Biosens Bioelectron* 79:280–287
 14. Hernández LA, del Valle MA, Díaz FR, Fermin DJ, Risbridger TAG (2015) Polymeric nanowires directly electrosynthesized on the working electrode. *Electrochim Acta* 166:163–167
 15. East GA, del Valle MA (2000) Easy-to-make Ag/AgCl reference electrode. *J Chem Edu* 77:97
 16. Hernandez LA, del Valle MA, Armijo FJ, Diaz FR, Louarn G (2013) Electro-oxidation of 1-amino-9,10-anthraquinone and o-phenylenediamine and the influence of its copolymerization in the modified electrode properties. *Electrochim Acta* 81:954–960
 17. Henstridge MC, Laborda E, Dickinson E, Compton RG (2012) Redox systems obeying Marcus–Hush–Chidsey electrode kinetics do not obey the Randles–Ševčík equation for linear sweep voltammetry. *J Electroanal Chem* 664:73–79
 18. Feng G, Xiong Y, Wang H, Yang Y (2008) Cyclic voltammetry investigation of diffusion of ferrocene within propylene carbonate organogel formed by gelator. *Electrochim Acta* 53:8253–8257
 19. Wang Y, Rogers EI, Compton RG (2010) The measurement of the diffusion coefficients of ferrocene and ferrocenium and their temperature dependence in acetonitrile using double potential step microdisk electrode chronoamperometry. *J Electroanal Chem* 648:15–19
 20. Moghaddam RB, Ali OY, Javashi M, Warburton PL, Pickup PG (2015) The effects of conducting polymers on formic acid oxidation at Pt nanoparticles. *Electrochim Acta* 162:230–236
 21. Habibi B, Delnavaz N (2010) Electrocatalytic oxidation of formic acid and formaldehyde on platinum nanoparticles decorated carbon-ceramic substrate. *Inter J Hydrogen Energy* 35:8831–8840
 22. Lović JD, Tripković AV, Gojković SL, Popović KD, Tripković DV, Olszewski P, et al. (2005) Kinetic study of formic acid oxidation on carbon-supported platinum electrocatalyst. *J Electroanal Chem* 581:294–302
 23. Marshall P, Glarborg P (2015) Ab initio and kinetic modeling studies of formic acid oxidation. *P Combust Inst* 35:153–160
 24. Gloaguen F, Leager J-M, Lamy C (1997) Electrocatalytic oxidation of methanol on platinum nanoparticles electrodeposited onto porous carbon substrates. *J Appl Electrochem* 27:1052–1060
 25. Ren F, Zhou W, Du Y, Yang P, Wang C, Xu J (2011) High efficient electrocatalytic oxidation of formic acid at Pt dispersed on porous poly (o-methoxyaniline). *Inter J Hydrog Energy* 36:6414–6421